Mon. Not. R. Astron. Soc. **000**, 000–000 (0000) Printed 9 June 1998 (MN LATEX style file v1.4)

Luminous and Dark Matter in the Milky Way

Rob P. Olling[1⋆], Michael R. Merrifield[1†]
[1] *Dept. of Physics and Astronomy,*
University of Southampton, Southampton SO17 1BJ, U.K.

9 June 1998

ABSTRACT

Strong interrelations exist between the Sun's distance to the Galactic centre (R_0), the local rotation speed (Θ_0), the stellar column density (Σ_*) and the shortest-to-longest axis ratio of the dark matter halo (q). In this paper we present simple analytical approximations that allow for an efficient search through the vastness of parameter space. We investigate the effects of the uncertain gaseous velocity dispersion (σ'_g) on the constraints imposed by the observed thickness of the Milky Way's H I layer. The extra degree of freedom resulting from the inclusion of the velocity dispersion parameter does not significantly alter the conclusions drawn in the accompanying paper regarding the interrelations between the Galactic constants, Σ_*, and q. A significant contribution to the total gas pressure by cosmic rays and magnetic fields beyond the optical disk is thus ruled out.

We find that the Milky Way's dark halo is close to spherical if $R_0 \gtrsim 7.1$ kpc, while a significantly flattened dark matter halo is only possible if our distance to the Galactic centre is smaller than ~ 6.8 kpc.

It is only possible to construct a self-consistent model of the Galaxy based on the IAU-recommended values for the Galactic constants ($R_0 = 8.5$ kpc, $\Theta_0 = 220$ km s^{-1}) if the effective gaseous velocity dispersion is larger than $\sim$10.8 km s^{-1} and if the local stellar column density is less than about 22 $M_\odot$ pc^{-2}. On the other hand, if we assume a value of Σ_* of 35 ± 5 $M_\odot$ pc^{-2} (Kuijken & Gilmore 1989b), we can rule out Galactic models with $R_0 \gtrsim 7.8$ kpc or $\Theta_0 \gtrsim 202$ km s^{-1}, whatever the value of σ'_g.

By analyzing the vertical force law in a self-consistent Galaxy model, we have uncovered a "vertical disk-halo conspiracy," which formalizes the well known fact that stellar kinematical data alone are insufficient to determine the column density of stars in the Solar neighbourhood. Combining the best kinematical and star-count estimates of Σ_*, we suggest that a value of $\Sigma_* = 32 \pm 11$ $M_\odot$ pc^{-2} is appropriate. We find that Kuijken & Gilmore's (1991) determination of the column density of matter within 1.1 kpc from the plane is robust and valid over a wide range of Galactic constants.

Our mass models show that, largely due to the uncertainty in the Galactic light distribution, the dark matter density in the Galactic centre is uncertain by up to three orders of magnitude. In the Solar neighbourhood this uncertainty is much reduced: our models imply a dark matter density of some 0.25 GeV/c^2 per cubic centimetre, or 0.0066 $M_\odot$ pc^{-3}– roughly 9% of the total mass density.

Key words: Galaxy: structure - Galaxy: kinematics and dynamics - Galaxy: solar neighborhood - Galaxy: fundamental parameters - Galaxy: stellar content

1 INTRODUCTION

The observational fact that rotation curves of external galaxies are rather flat in their outer parts (Rubin, Ford & Thon-

⋆ E-mail: olling@astro.soton.ac.uk
† E-mail: mm@astro.soton.ac.uk

© 0000 RAS

nard 1980; Bosma 1981; Kent 1987; Begeman 1987; Casertano & van Gorkom 1991; Broeils 1992; Persic, Salucci & Stel 1996) suggests the presence of unseen matter in those galaxies[‡]. The same holds for the Milky Way. A fit to the observed rotation curve can be used to yield the stellar mass-to-light ratio $\Upsilon_{\rm d}$, and the dark halo parameters, albeit with large uncertainties. Rather than using this fitting procedure, we adopt an analytical approximation in which there is only one free parameter: the degree to which the disk is maximal (γ), from which $\Upsilon_{\rm d}$ and the dark halo parameters follow (see Olling 1995 for details). The parameter γ is preferred for dynamical modeling purposes as it is bound between 0 and 1, zero mass and "maximum disk", respectively. For example, in the popular "maximum-disk" hypothesis (van Albada & Sancisi 1986), the amplitude of the stellar rotation curve equals $(85 \pm 10)\%$ of the observed rotation speed (Sackett 1997), so that $\gamma = 0.85$. In contrast, Bottema (1993) used stellar velocity dispersion measurements to "weigh" stellar disks, and concluded that they are sub-maximal, with $\gamma = 0.63 \pm 0.1$. The situation is similarly indeterminate for the Milky Way: the Kuijken & Gilmore (1989) model implies $\gamma \sim 0.5$, while more recent models with lower rotation speed and shorter scale-lengths can be close to maximal ($\gamma = 0.85 \pm 0.1$; Sackett 1997). As a result of the uncertain stellar mass-to-light ratio, the dark halo parameters are very ill determined for most galaxies (e.g., van Albada & Sancisi 1986; Lake & Feinswog 1989; Olling 1995; Table 1). The Milky Way is no different: the combined uncertainty in the local disk mass and the stellar scale-length introduces an uncertainty of over three orders of magnitude in the central dark matter (DM) density of the Milky Way, and about an order of magnitude uncertainty in its core radius (see also Dehnen & Binney 1998).

In the Solar neighborhood the situation is less dramatic, although no consensus exists on the local volume density of dark matter [the Oort limit, see Crézé *et al.* (1998) for a recent review]. However, the local dark matter density is extremely important for many problems in astrophysics. For example, if the dark matter comprises elementary particles like neutralinos, axions, WIMPS etc., their expected detection rate is proportional to the DM density or its square, depending on whether the particles themselves or their annihilation products are searched for. Likewise, if the dark halo is made up of massive compact halo objects (MACHOs), the event rate for gravitational lensing depends on the integrated dark matter density along the line of sight towards the lens. Furthermore, in the accompanying paper (henceforth Paper I) we show that measurements of the amount of dark matter in the Galactic midplane can be used to place tight constraints on the Sun's distance of the Galactic centre, and the local Galactic rotation speed. These constraints in turn affect the predicted micro-lensing time scales and optical depths (Gates, Gyuk & Turner 1995), and the expected neutralino annihilation signal (Bergstrom, Ullio & Buckley 1997).

In an ideal world, parameters such as the Sun's distance to the Galactic centre (R_0), the rotation curve [$\Theta(R)$], the local rotation speed (Θ_0), the scale-length of the optical disk ($h_{\rm R}$), the local stellar column density (Σ_*), the gaseous velocity dispersion (σ_g) and so forth, are not only measured, but also have normal errors. In that case one could determine other quantities that depend on these parameters by comparing the model and observed parameters in a χ^2 sense. Unfortunately, the quoted errors on R_0, Θ_0, etc. are not normal, and the values themselves are not averages in the statistical sense (see Paper I).

However, strong interrelations exist between the parameters that describe a particular mass model, so that their values cannot be chosen arbitrarily (Paper I). In this paper we further explore how the "observed" values of R_0, Θ_0, $h_{\rm R}$, Σ_*, and σ_g and the uncertainties therein affect our ability to infer the distribution of dark matter in the Milky Way. We seek models that can reproduce two observables sensitive to the DM density: the amount of mass within 1.1 kpc of the Galactic midplane at the Solar circle, and the radial increase of the thickness of the H I layer or "flaring." In order to do so we construct several mass models for the Milky Way with properties that span the allowed ranges of the Galactic constants (R_0=6.8, 7.1, 7.8, and 8.5 kpc, with Θ_0=182, 189, 207, and 227 km s^{-1}, respectively), the scale-length of the stellar disk ($h_{\rm R}$=2, 2.5, and 3 kpc), and the stellar disk mass with $\Upsilon_{\rm d}$ such that Σ_*=35 $\pm$ 10 $M_\odot$ pc^{-2}. To calculate model flaring curves, we use the algorithm developed by Olling (1995) to determine the radial and vertical force laws self-consistently by integration over the density distribution of the entire Galaxy. This procedure is rather expensive[§], so we use this method only for the limited number of models described above. For a more complete investigation of parameter space we use the approximation described in §4.2.

Because the mass of the stellar disk proves to be a powerful constraint on the mass models, we investigate the reliability of its determination. In agreement with many previous results, we find that the kinematically-determined stellar column density is extremely ill determined if no rotation curve constraint is applied. We also confirm Kuijken & Gilmore's (1991; hereafter referred to as KG91) result that the *total mass* column density within about 1 kpc of the plane is rather tightly constrained, for a wide range of Galactic constants. Since the dark matter density is larger for models with larger values of Θ_0 or more highly flattened halos, it follows that strong correlations must exist between the mass of the stellar disk, the local rotation speed and the

[‡] See McGaugh & de Blok (1998) for a review of the alternative hypothesis that the law of gravity has to be modified instead.

[§] Each choice of R_0 and Θ_0 , requires the re-determination of the H I and H_2 radial column density distributions as well as the observed thickness of the H I layer (see below), a process that is not easily automated. Further, the calculation of model gas layer widths for a given combination of R_0, Θ_0, $\Upsilon_{\rm b}$, $h_{\rm R}$ and $\Upsilon_{\rm d}$ takes about 1.3 hours per q-values, on a 50 MHz dual processor SPARC-10.

halo's flattening. Including constraints from the thickness of the H I layer in the outer Galaxy allows for the determination of very tight relations between all the mass models' parameters.

The results presented in Paper I were based on the assumption that the gas layer beyond the optical disk can be adequately represented by a single, iso-thermal component: the warm neutral phase. There we also presented theoretical and observational arguments to support that assumption. In the present paper we will test another critical assumption made in Paper I, namely that non-thermal pressures provide negligible support for the H I layer beyond the optical disk.

The structure of this paper is as follows. In the next section we describe the components that comprise our mass models, determine the dark matter density in the Solar neighborhood, and present the radial dark matter distribution of the Milky Way. In §3 we compare star count and kinematical methods to determine the local stellar column density. In §4 we present two new methods that can be used to constrain the Milky Way's dark matter density distribution. Simple analytical models that describe the relation between the dark matter density in the Solar neighbourhood, the halo's shape, and the Galactic constants are presented in §4.1. At larger distances, the dark matter density is constrained significantly by observations of the thickness of the H I layer (§4.2). We investigate the effects of possible non-thermal pressure support for the H I layer in §5. We summarize and conclude in §6.

2 THE MASS COMPONENTS

In this section we describe in more detail the components included in our mass models of the Milky Way: the stellar bulge and disk, the gas layer, and the dark halo. When quantifying these components using parametric models, it is important to realize that the values of the parameters will depend upon the choice of the Galactic constants.

We base our model for the bulge on Kent's (1992) K-band luminosity distribution. The bulge is a modified spheroid with "boxy" appearance: $\rho_{Bulge}(s) = 3.53 K_0(s/[667\ \mathrm{pc}])\ L_{\odot,K}\ \mathrm{pc}^{-3}$, with $s^4 = R^4 + (z/0.61)^4 + 10^4$. Throughout this paper we use cylindrical coordinates with R the Galactocentric distance, and z the distance of the plane. The bulge is flattened with axial ratio 0.61. To avoid the singularity of the K_0-Bessel function at $s = 0$, we include a softening of 10 pc, which leads to a central luminosity density of 15.24 $L_{\odot,K}\ \mathrm{pc}^{-3}$. Beyond 3 kpc we truncate the bulge exponentially with a scale-length of 133 pc.

For the disk, we use the standard form of a radially exponential disk with scale-length h_R. For its vertical distribution we use a secant-hyperbolic function, which is a compromise between the often used exponential and secant-hyperbolic-squared forms (van der Kruit 1988). For simplicity, the exponential scale-height (z_e) of the disk is taken to be constant at 300 pc, intermediate between the values suggested by Kent (1992) and Reid & Majewski (1993). The stellar disk is truncated at $(R_0 + 4.5)$ kpc (Robin, Crézé & Mohan 1992; Freudenreich 1996, 1998).

Because of our location inside the Galaxy, the numerical values of the scale-length, the scale-height, the projected surface brightness, and the face-on central surface brightness [$L_{\mathrm{d,K}}(0)$] for the disk depend upon the assumed value of our distance to the Galactic centre. From Freudenreich (1996, 1998) we find that these quantities typically increase with R_0, by 8%$\times$ (R_0/kpc - 8). Such variations induce a change in total luminosity which is a factor of three larger. Because these corrections are smaller than the ones resulting from the uncertainty in h_R (see below), we do not apply these corrections. Given the wide range of values for the stellar scale-lengths circulating in the literature (Sackett 1997), we consider models with stellar scale-lengths of h_R=2, 2.5, and 3 kpc, which bracket Freudenreich's value. For any given R_0, the total luminosity is better determined than either central surface brightness or scale-length (Kent, Dame & Fazio 1991). Thus, we scale the K-band central surface brightness such that the total luminosity is conserved for each choice of h_R [$L_{\mathrm{d,K}}(0)$ =2200, 1408, and 978 $L_{\odot,K}\ \mathrm{pc}^{-2}$, for h_R=2, 2.5, and 3 kpc, respectively]. Further, for each choice of h_R we chose a K-band mass-to-light ratio ($\Upsilon_{\mathrm{b,K}}$) for the bulge such that a large range in the mass-to-light ratio for the disk ($\Upsilon_{\mathrm{d,K}}$) is allowed. Kuijken & Gilmore (1989b, hereafter referred to as KG89) found the mass of the stellar disk to be Σ_*= 35 $\pm$ 5 $M_\odot\,\mathrm{pc}^{-2}$. We adopt values for the disk mass-to-light ratios so as to span the 2-σ range in Σ_*.

We now turn to the contribution to the mass models from the interstellar medium (ISM). Our location inside the Milky Way means that we cannot determine distances to diffuse components like the ISM directly. Instead, we must infer the distance by comparing the observed radial velocity of the material with the predictions of a kinematical model. Thus, important properties like scale-height, column density, and total mass of the ISM depend on the Galactic constants and the Milky Way's rotation curve (see also Paper I). Thus, we re-determine the atomic and molecular gas distributions for each choice of R_0 and Θ_0 . While the column densities at fractional radius R/R_0 are independent of the choice of R_0 & Θ_0 (Bronfman *et al.* 1988), the total gas mass and the thickness of the gas layer are not. For the inner Galaxy, the H I column density was determined from the midplane volume density (Burton 1988) and the observed thickness of the layer (Malhotra 1995). The H I column densities for $R \gtrsim R_0$ were taken from Wouterloot *et al.* (1990), with 9.25 $M_\odot\,\mathrm{pc}^{-2}$ at the Solar circle. The H_2 column densities for the inner and outer Galaxy were taken from Bronfman *et al.* (1988) and Wouterloot *et al.* (1990), respectively. The column density of H_2 at the Solar circle is 1.8 $M_\odot\,\mathrm{pc}^{-2}$, and so, neglecting the column density due to the other phases of the ISM, we arrive at a total column density at the Solar circle of Σ_{ISM}=14.5 $M_\odot\,\mathrm{pc}^{-2}$, which includes 23.8% helium by mass (Olive & Steigman 1995). A graphical representation of the derived gaseous surface density distributions can be found in a related paper on the Galactic & Oort constants (Olling & Merrifield 1997a,1998b). We present the radial increase of the thickness of the gas layer in Paper I. The

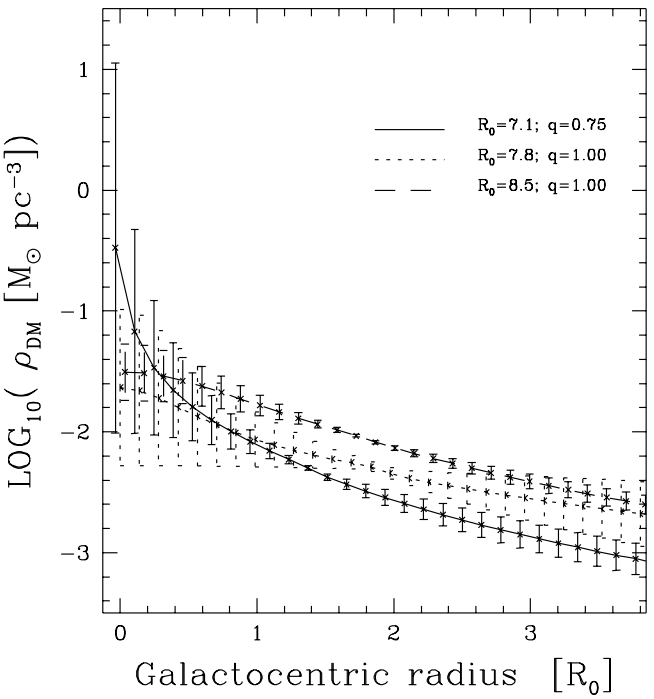

Figure 1. The dark matter midplane density distribution calculated using equation (1) for three values of R_0 and q. The densities scale approximately as $1/q$ (Olling 1995) The error bars represent the full range for the case corresponding to $\Sigma_* = 35 \pm 5\ M_\odot\,\mathrm{pc}^{-2}$, and h_R=2 to 3 kpc. Notice that although the DM density at the Solar circle is relatively well determined, the central density is uncertain by more than three orders of magnitude. Note that we have offset the radial coordinates of the R_0=7.1, and 8.5 kpc models from their true positions (i.e., the R_0=7.8 kpc points) to avoid overlapping symbols.

midplane densities of the atomic and molecular hydrogen at the Solar circle can be found from the column density and thickness of these components. The width of the H I and H_2 components are 410 ± 30 pc, and 141 ± 20 pc, respectively (Paper I). We thus find $\rho_{\mathrm{H\,I}}(R_0) = (21 \pm 1.5)\ 10^{-3}$, and $\rho_{\mathrm{H_2}}(R_0) = (12 \pm 1.5)\ 10^{-3}\ M_\odot\,\mathrm{pc}^{-3}$. Including the He correction, we find a local volume density for the ISM of $\rho_{ISM}(R_0) = (43 \pm 3)\ 10^{-3}\ M_\odot\,\mathrm{pc}^{-3}$.

As is commonly done (e.g., van Albada & Sancisi 1986; Kent 1987; Begeman 1989; Lake & Feinswog 1989; Sackett & Sparke 1990; Broeils 1992; Olling 1995; Olling 1996b), we model the dark matter density distribution as a non-singular isothermal spheroid with flattening q, and a density distribution given by:

$$\rho_h(R,z;q) \quad = \quad \rho_0 \left(\frac{{R_c}^2}{{R_c}^2 + R^2 + (z/q)^2} \right) , \qquad (1)$$

where the halo's core radius (R_c) and central density (ρ_0) depend on the flattening in such a way that the family of density distributions $\rho_h(q)$ have a rotation curve that is essentially independent of q (Olling 1995).

Figure 1 shows the radial distribution of dark matter for three values of R_0, and the range in model parameters as listed in Table 1. Each choice of the stellar scale-length and local column density of stars results in a different distribution. The largest DM densities are obtained for large scale-lengths and small values of Σ_*. Even though the central DM density is uncertain by over three orders of magnitude, the local dark matter density is determined rather well: we find

$$\frac{\rho_{\mathrm{DM}}(R_0,\Theta_0)}{10^{-3} M_\odot\,\mathrm{pc}^{-3}} \quad = \quad \frac{10 + 7 \times (R_0 - 7.8) \pm 2}{q\,(26.7 R_0/\Theta_0)^2} \qquad (2)$$

where R_0 is in kpc, and Θ_0 in km s^{-1}. The ($\sim 25/q$)% uncertainty arises as a result of the uncertainty in $\Sigma^{tot}_{1.1}$, the total column density within 1.1 kpc of the plane [71 ± 6 $M_\odot\,\mathrm{pc}^{-2}$, (Kuijken & Gilmore 1991)], and the uncertainties in the values for the stellar and ISM disk masses presented above.

With these ingredients, we compute the exact vertical and radial force laws for a limited number of models as described in the Introduction. We present a log for a representative sample of the models in Table 1.

2.1 Other mass models

Of course, other mass models can be constructed which represent the dark matter density distribution (eg; van Albada & Sancisi 1986; Navarro, Fren & White 1996; Dehnen & Binney 1998). However, all viable mass models must share the property that they reproduce the Galactic rotation curve. For a round halo the vertical force approximately equals z/R times the radial force. Since the radial force is the approximately the same for all models which reproduce the observed rotation curve, the ensemble of possible models also have approximately equal vertical forces, independent of the exact radial DM density distribution (Olling 1995; Olling 1997c). In a flattened halo with the same rotation curve, the DM densities are roughly proportional to $1/q$, independent of the radial mass distribution. The thickness of the gas layer is thus proportional to $\sqrt{q}$ [cf. eqns. (18) and (20)], independent of the detailed form of $\rho_h(R)$. Thus, our analysis will not be seriously compromised by restricting ourselves to one particular DM density distribution.

3 THE LOCAL STELLAR COLUMN DENSITY: A CONSTRAINT?

The Milky Way is a unique galaxy in that we can, at least in principle, determine the local column density of stars directly. Once Σ_* is accurately determined, it is possible to establish to what degree the Milky Way disk is maximal, which would provide an important benchmark for external galaxies. Unfortunately this benchmark is not yet available, as the values for Σ_* reported in the literature range from 26 to 145 $M_\odot\,\mathrm{pc}^{-2}$.

From simple analytic arguments (§4.1) it follows that

Table 1. Disk & halo parameters. The meaning of the columns is as follows: 1) γ, the degree to which the stellar disk is maximal; 2) scale-length of stellar disk (kpc); 3&4) bulge & disk K-band mass-to-light ratios; 5&6) stellar column density & total column density within 1.1 kpc of the plane ($M_\odot\,\mathrm{pc}^{-2}$); 7&8) core radius (kpc) and central density ($10^{-3}\ M_\odot\,\mathrm{pc}^{-3}$) of the dark halo, assuming q=1 (multiply by $\approx 1/q$ to scale to different values of q, for a more exact scaling, see Olling 1995); 9&10) dark halo flattening as inferred from the H I flaring ($q_{\mathrm{H\ I}}$) and the local column densities ($q_{1.1}$). The face-on K-band central surface brightness of the disk is 2200, 1408, and 978 $L_\odot\,\mathrm{pc}^{-2}$, for h_R=2, 2.5, and 3 kpc, respectively. The total K-band disk & bulge luminosities are 5.5×10^{10} and $1.5\times10^{10}\ L_\odot$. The Milky Way's K-band bulge-to-disk ratio, 0.27, is within the expected range of galaxies of its type (de Jong 1996). Strictly speaking, the surface adopted brightness, mass-to-light ratio, scale-height and scale-length are only compatible with the Milky Way's photometry for R_0 = 8 kpc, the value used by Kent (1992).

γ	h_R	$\Upsilon_{\mathrm{b,K}}$	$\Upsilon_{\mathrm{d,K}}$	Σ_*	$\Sigma_{1.1}^{tot}$	R_c	ρ_0	$q_{\mathrm{H\ I}}$	$q_{1.1}$
R_0=6.8									
0.80	2.0	0.55	0.422	30.21	62.48	2.39	73.8	0.630 ± 0.107	0.561 ± 0.175
0.86	2.0	0.55	0.488	34.92	66.02	3.54	35.6	0.687 ± 0.113	0.664 ± 0.226
0.92	2.0	0.55	0.558	39.96	68.72	6.09	14.6	0.699 ± 0.120	0.753 ± 0.295
0.64	2.5	0.55	0.327	29.58	63.56	1.32	246.3	0.687 ± 0.152	0.620 ± 0.183
0.70	2.5	0.55	0.392	35.39	68.84	1.86	125.1	0.717 ± 0.134	0.826 ± 0.268
0.75	2.5	0.55	0.449	40.63	73.40	2.45	73.0	0.674 ± 0.127	1.061 ± 0.371
0.56	3.0	0.55	0.306	30.21	64.34	0.70	853.9	0.740 ± 0.181	0.651 ± 0.194
0.60	3.0	0.55	0.351	34.68	68.6	1.00	421.0	0.770 ± 0.159	0.820 ± 0.261
0.65	3.0	0.55	0.412	40.70	74.18	1.44	201.9	0.762 ± 0.137	1.114 ± 0.382
R_0=7.1									
0.82	2.0	0.45	0.482	29.71	61.94	2.73	62.7	0.625 ± 0.132	0.544 ± 0.165
0.89	2.0	0.45	0.568	35.00	65.66	4.53	25.5	0.624 ± 0.116	0.636 ± 0.214
0.95	2.0	0.45	0.647	39.87	66.74	9.77	8.6	0.679 ± 0.104	0.603 ± 0.239
0.65	2.5	0.55	0.370	29.66	62.60	1.13	340.1	0.727 ± 0.159	0.581 ± 0.173
0.71	2.5	0.55	0.441	35.39	67.76	1.66	158.2	0.738 ± 0.161	0.765 ± 0.250
0.76	2.5	0.55	0.506	40.55	72.26	2.25	86.4	0.823 ± 0.223	0.999 ± 0.356
0.56	3.0	0.55	0.333	29.73	61.82	0.20	9884.5	0.735 ± 0.181	0.550 ± 0.168
0.61	3.0	0.55	0.395	35.28	67.10	0.55	1343.6	0.703 ± 0.158	0.734 ± 0.243
0.63	3.0	0.55	0.421	37.63	69.32	0.71	802.8	0.786 ± 0.210	0.843 ± 0.290
R_0=7.8									
0.92	2.0	0.45	0.687	29.80	64.60	9.51	15.4	1.003 ± 0.119	0.616 ± 0.162
0.72	2.5	0.75	0.492	29.80	64.76	4.59	47.9	1.744 ± 0.553	0.963 ± 0.240
0.78	2.5	0.75	0.577	34.97	71.00	5.81	32.6	1.616 ± 0.443	1.065 ± 0.260
0.84	2.5	0.75	0.669	40.56	77.66	8.01	20.6	1.461 ± 0.337	1.191 ± 0.331
0.59	3.0	0.75	0.430	30.46	66.54	2.84	103.4	1.623 ± 0.451	0.973 ± 0.244
0.61	3.0	0.75	0.460	32.56	68.06	3.02	91.7	2.019 ± 0.758	1.026 ± 0.260
0.68	3.0	0.75	0.572	40.46	77.54	3.81	59.3	1.810 ± 0.753	1.327 ± 0.364
R_0=8.5									
0.76	2.5	0.60	0.670	30.66	78.68	6.81	39.1	2.922 ± 0.863	1.169 ± 0.252
0.81	2.5	0.60	0.761	34.83	80.43	8.34	28.9	2.512 ± 0.608	1.228 ± 0.279
0.86	2.5	0.60	0.857	39.26	81.28	11.10	19.9	1.931 ± 0.366	1.256 ± 0.306
0.59	3.0	0.85	0.486	27.23	76.53	5.09	60.2	1.424 ± 0.156	1.165 ± 0.193
0.67	3.0	0.85	0.627	35.11	82.49	6.20	43.2	1.498 ± 0.183	1.364 ± 0.213
0.75	3.0	0.85	0.785	44.00	88.53	8.07	28.9	1.475 ± 0.197	1.641 ± 0.159

the inferred *shape* of the Milky Way's dark matter halo depends strongly on the actual mass of the stellar disk. These arguments can be extended to show that tight correlations exist between the Galactic constants, Σ_*, the halo's flattening (Paper I), and the velocity dispersion of the H I layer (§5). Therefore, it is essential to narrow down the wide range in stellar disk masses reported in the literature. Below we try to assess the accuracy of the reported values.

Two basic techniques have been employed to determine Σ_*. The direct method involves converting star counts as a function of Galactic coordinates and magnitude to in-situ mass densities. This method is somewhat hampered by uncertainties in the conversion from luminosity to mass,

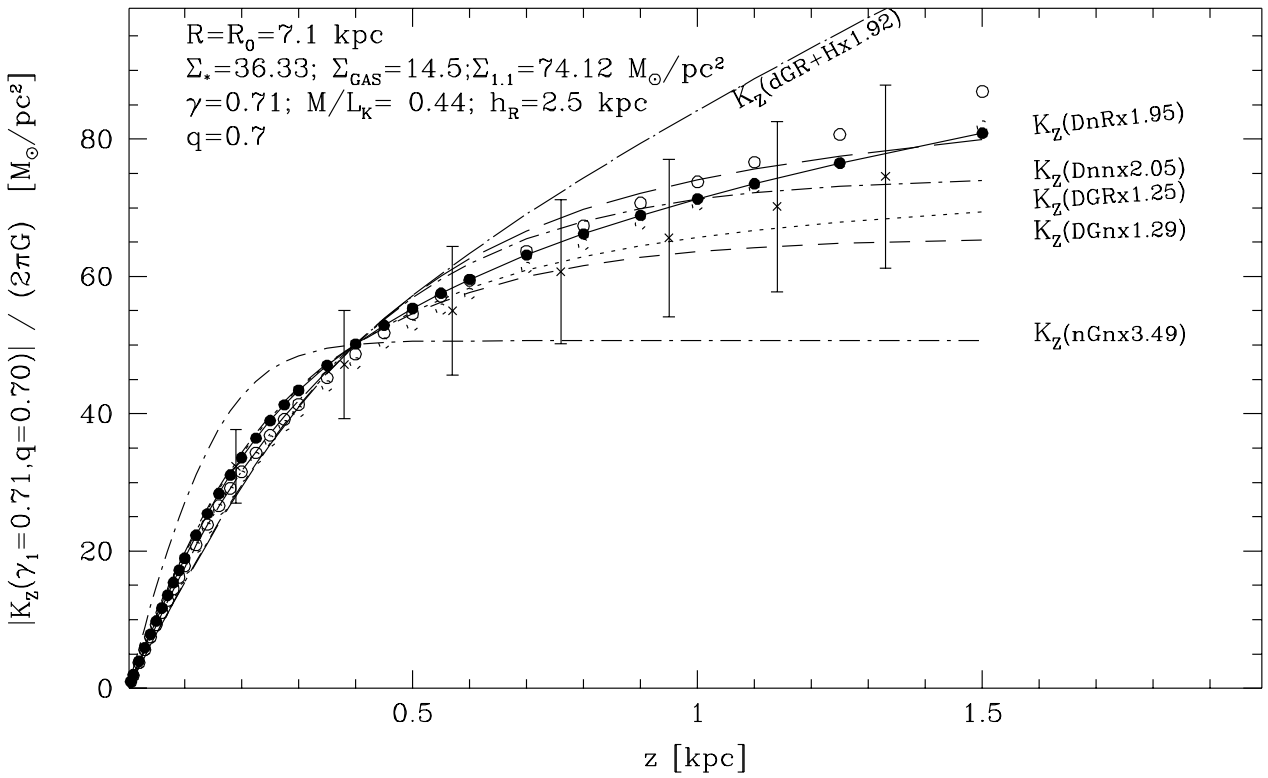

Figure 2. We present the exact vertical force (filled circles) at Galactocentric distance R_0 for a model that almost reproduces the values for Σ_* and $\Sigma_{1.1}^{tot}$ proposed by Kuijken & Gilmore (1989, 1991). The local approximation to the exact force law that uses the slope of the rotation curve (open circles) or assumes a flat rotation curve (dashed open circles) are also indicated. Some other models in which the DM is distributed like various superpositions of the known components are also plotted: 1) $\rho_{DM} = 1.29 \times (\rho_* + \rho_g)$ (labeled "DGnx1.29"); 2) $\rho_{DM} = 1.25 \times (\rho_* + \rho_g + \rho_{rot})$ ("DGRx1.25"); 3) $\rho_{DM} = 2.05 \times \rho_*$ ("Dnnx2.05"); 4) $\rho_{DM} = 1.95 \times (\rho_* + \rho_{rot})$ ("DnRx1.95"); 5) $\rho_{DM} = 3.49 \times \rho_g$ ("nGnx3.49"). For the curve labelled "dGR+Hx1.92" we used a smaller column density of stars 25.8 $M_\odot$ pc^{-2} (Gould, Bahcall & Flynn 1997), and multiplied the halo contribution by 1.92. Most of the models have very similar force laws in the region close to the plane (see also Table 2). We also include KG89's vertical force law and the errors thereupon (crosses with error bars).

completeness problems in the Solar neighborhood, and binary corrections at large distances. Gould, Bahcall & Flynn (1997; hereafter referred to as GBF97) used deep HST star counts of M-dwarfs at great heights above the plane in combination with a local normalization to infer a stellar column density of only $\Sigma_* = 25.8 \pm 3.8\ M_\odot\,\mathrm{pc}^{-2}$.

The second, kinematical, method employs the interrelationship between the potential, the vertical density distribution, and the variation of the velocity dispersion with z. Many authors have employed this method, yielding a large range in inferred values for Σ_*. For example, Bahcall (1984b) found Σ_* values of ∼40, ∼52, ∼68, and ∼145 $M_\odot\,\mathrm{pc}^{-2}$ for dark matter distributions that resemble the gaseous disk, an isothermal halo, the thin stellar disk, or the thick stellar disk, respectively. Other authors find values as low as 35 $M_\odot\,\mathrm{pc}^{-2}$ (Kuijken & Gilmore 1989b; Flynn & Fuchs 1994). Methods that combine the two primary methods exist as well (Bienaymé, Robin & Crézé 1987; Crézé, Robin & Bienaymé 1989).

We investigate the accuracy of the kinematic determination of the stellar column density with the aid of Galaxy models for which we calculate the exact force law from the known global distribution of matter. The model for which we carry out this investigation has the following parameters: R_0 =7.1 kpc, Θ_0 =189 km s^{-1}, $h_{\rm R}$=2.5 kpc, q=0.7, and γ=0.71, which yield Σ_*=36.5 and $\Sigma_{1.1}^{tot}$=74.1 $M_\odot\,\mathrm{pc}^{-2}$. These values lie close to the best estimates for the Milky Way (Kuijken & Gilmore 1989, 1991; Olling & Merrifield 1998b). We also investigate the validity of an often used approximation to the total force. This local approximation treats the disk as a parallel slab of infinite extend and constant surface density. In that paradigm, the vertical force law can be derived from the Poisson equation by performing a vertical integration of the effective matter density, which includes matter and rotation curve gradient terms [ρ_m and $\rho_{rot} \equiv \frac{-2}{4\pi G}\frac{V_{rot}}{R}\frac{dV_{rot}}{dR}$, respectively; (Olling 1995)]:

$$K_{z,\mathrm{local}}(z) \quad = \quad -4\pi G \int_0^z dz' \left[\rho_m(z') + \rho_{rot}\right] , \qquad (3)$$

Table 2. The accuracy to which various erroneous matter distributions, ρ_{err}, can reproduce the true vertical force. The first four columns describe that ρ_{err} was used: $\rho_{err} = X_d \times \rho_d + X_g \times \rho_g + X_{rot} \times \rho_{rot} + X_h \times \rho_h$. The last three columns indicate the average ratio of $K_{z,true}/K_{z,err}$ over the vertical ranges indicated [0 - 0.4 kpc (Z1), 0.4 - 0.8 kpc (Z2), and 0.8 - 1.2 kpc (Z3)]. The typical variation within these radial ranges is a few %, except for the gas-only case where it can be up to 35%. We also indicate the inferred stellar column density (Σ_*') and total column within 1.1 kpc of the plane ($\Sigma_{1.1}'$), in units of $M_\odot\,\mathrm{pc}^{-2}$. The last two lines give the average and standard deviations of the lines above (excluding the gas-only model).

X_d	X_g	X_{rot}	X_h	Z1	Z2	Z3	Σ_*'	$\Sigma_{1.1}'$
1.25	1.25	1.25	0.00	1.03	0.99	0.93	45.4	63.6
1.29	1.29	0.00	0.00	0.95	1.04	1.17	46.9	65.6
2.05	0.00	0.00	0.00	0.85	1.03	1.01	74.5	74.5
1.95	0.00	1.95	0.00	0.85	1.03	1.04	70.8	70.8
0.00	3.49	0.00	0.00	1.35	0.90	0.72	0.0	50.6
1.40	1.00	1.00	0.03	1.03	0.99	0.93	50.9	66.1
1.25	1.00	1.00	0.46	1.03	0.99	0.93	45.4	70.6
1.00	1.00	1.00	1.17	0.97	1.02	1.08	36.3	78.1
0.74	1.00	1.00	1.92	0.95	1.04	1.17	26.9	86.1
0.50	1.00	1.00	2.59	0.93	1.06	1.24	18.2	92.9
0.25	1.00	1.00	3.30	0.92	1.08	1.33	9.1	100.4
0.12	1.00	1.00	3.67	0.91	1.09	1.37	4.4	104.3
							39± 58%	77± 21%

with G Newton's constant of gravity, and K_z the vertical force per unit mass.

In Fig. 2 we present true vertical force (filled circles) and the local approximation (open circles). We see that in the Solar neighborhood and close to the plane, the local approximation is reasonably accurate[¶] and can be used as an approximation to the true vertical force law. We also include the observationally determined K_z [crosses with error bars; KG89's equation (1) with D=250 pc]. The Galactic constants we are using here lie at the extreme end of the models investigated by Kuijken & Gilmore. However, we find that other models, within the 1-σ range of Θ_0/R_0 , h_R, Σ_*, and $\Sigma_{1.1}^{tot}$, yield similar results. That is to say, the vertical force law in all our Galaxy models are compatible with KG91's, implying that their results can be directly applied here.

Now we investigate the possibility that the actual dark matter density law differs from the distribution in our models [eqn. (1)]. Choosing a different DM distribution while keeping the observed K_z fixed requires a different luminous mass distribution. As a simple test case, we plot a model where the DM density is multiplied by 1.92 (labelled "dGR+Hx1.92" in Fig. 2). In this case, we have to decrease the stellar column density to the GBF97 value (25.8 $M_\odot\,\mathrm{pc}^{-2}$) in order to keep K_z approximately unchanged. Next we consider DM distributions inspired by Bahcall's "P" models (1984b), where the DM density is assumed to be proportional to that of a known component. The accuracy to which the true vertical force is reproduced by these various alternative DM density distributions is summarized in Table 2. In this table we also include models in which we change the stellar column density and scale the DM density such that the force at 400 pc above the plane equals the true value. The lower part of the table shows that it is possible to decrease Σ_* by more than an order of magnitude and simultaneously increase ρ_h without altering $K_z(|z| \leq 800\mathrm{pc})$ substantially: this amounts to a "vertical disk-halo conspiracy." However, in a self-consistent treatment of the problem one cannot change the disk mass arbitrarily, as the rotation curve imposes a constraint as well.

From the data presented in Table 2 it is clear that, without additional assumptions, stellar kinematical data extending to a few hundred parsecs are not sufficient to determine the mass of the stellar disk. However, the total mass within 1.1 kpc of the plane is much better determined, in agreement with Kuijken & Gilmore (1991). In order to discriminate between models, it is essential to incorporate a rotation curve constraint. Kuijken & Gilmore (1989) used such a constraint explicitly, while Bahcall (1984b) and Flynn & Fuchs (1994) used "reasonable" values for the density of non-disk-like dark matter to rule out extreme values for the mass of the stellar disk.

Furthermore, if data at larger z are considered, the differences between the force laws shown in figure 2 start to become apparent. For example, Flynn & Fuchs (1994) used the density distribution of K-giants at high z to exclude disk column densities above 68 $M_\odot\,\mathrm{pc}^{-2}$. To determine the stellar column density from stellar kinematics, one *has* to include rotation curve constraints and sample the region above 1 kpc.

Considering the uncertainties in the kinematical estimates of the total mass of the disk, it appears to be preferable to use the direct star count method to determine Σ_*. The latest results by GBF97 imply Σ_*=25.8 ± 3.8 $M_\odot\,\mathrm{pc}^{-2}$. However, the local space density of stars found by these authors [$\rho_* = (33.2 \pm 8.6)\ 10^{-3}\ M_\odot\,\mathrm{pc}^{-3}$] is somewhat lower than values reported in the literature. Wielen (1974) finds $\rho_* = 46\ 10^{-3}\ M_\odot\,\mathrm{pc}^{-3}$, Bahcall (1984a) uses $\rho_* = 50.8\ 10^{-3}\ M_\odot\,\mathrm{pc}^{-3}$, and from Crézé *et al.* (1998) we infer[‖]: $\rho_* = (26 \pm 15)\ 10^{-3}\ M_\odot\,\mathrm{pc}^{-3}$. This suggests that GBF97 underestimated Σ_* by a factor of 1.24 ± 0.4, and so we find $\Sigma_* = 32 \pm 11\ M_\odot\,\mathrm{pc}^{-2}$, which is remarkably close to

[¶] For the ensemble of models for which the parameters differ by $\leq$ 1-σ from the model presented here, the approximations based on equation (3) reproduce the true K_z typically to within **7%**: sometimes models that include the rotation curve gradient term perform best, sometimes not.

[‖] From their value for the total volume density [$\rho_{tot} = (76 \pm 15)\ 10^{-3}\ M_\odot\,\mathrm{pc}^{-3}$], we subtract our ISM volume density [$(43 \pm 3)\ 10^{-3}\ M_\odot\,\mathrm{pc}^{-3}$, §2] and the contribution from the extended DM halo distribution [$(7 \pm 3)\ 10^{-3}\ M_\odot\,\mathrm{pc}^{-3}$, eqn. (2) with $R_0 = 7.1$ kpc, $\Theta_0 = 189\,\mathrm{km\,s}^{-1}$, $q = 0.75$] to arrive at $\rho_* = (26 \pm 15)\ 10^{-3}\ M_\odot\,\mathrm{pc}^{-3}$.

the kinematical estimates of Flynn & Fuchs (1994; Σ_*=37 $\pm$ 13 $M_\odot\,\mathrm{pc}^{-2}$) and KG89 ($\Sigma_*$=35 $\pm$ 5 $M_\odot\,\mathrm{pc}^{-2}$).

To summarize the above: we confirm Kuijken & Gilmore's (1991) conclusion that the total mass within 1.1 kpc of the Galactic midplane is a well determined quantity in the Solar neighbourhood. Mass models for the Milky Way *have* to conform to the constraint $\Sigma_{1.1}^{tot}$= 71 $\pm$ 6 $M_\odot\,\mathrm{pc}^{-2}$. We also find that this constraint is valid for a wide range in Galactic constants. The mass of the stellar disk is less well determined: Σ_*= 32 $\pm$ 11 $M_\odot\,\mathrm{pc}^{-2}$ encompasses the best star count and kinematical determinations. Subtracting the column densities of the stellar and ISM distributions, dark matter in the Solar neighbourhood amounts to 24.5 $\pm$ 11 $M_\odot\,\mathrm{pc}^{-2}$ within 1.1 kpc of the plane.

4 FURTHER CONSTRAINTS ON THE DARK MATTER DENSITY

In this section we present two simple analytical models to illustrate the relation between the Galactic constants, the mass of the stellar disk, the velocity dispersion of the gas layer, thickness of the gas layer, and the dark halo's flattening. These models can be used to show how information obtained from measurements of the local stellar kinematics constrain the dark matter density at $R = R_0$, while the width of the gas layer limits the DM density at $R \sim 2R_0$.

4.1 Constraints from the local stellar kinematics

Kuijken & Gilmore (1991) asserted that the kinematics of stars in the Solar neighbourhood cannot be used to determine the local volume density of dark and luminous matter to high accuracy. However, as we have seen above, these stellar kinematical constraints can be used to accurately determine the total mass within 1.1 kpc of the Galactic plane.

Because the contribution of the stellar and dark matter components cannot be clearly segregated, their inferred column densities are highly correlated: a low stellar column density implies a large amount of dark matter, and vice versa. Since the dark matter density depends on the amplitude of the rotation curve and the halo's flattening, these parameters are in turn related to Σ_*. Below we investigate these relations in some detail.

Integrating equation (1) with respect to z and applying equation (A4) from Olling (1995), we find the column density of dark matter within z of the Galactic plane as a function of q:

$$\Sigma_{h,z}(q) \;=\; \frac{2\rho_0 q R_c^2}{\sqrt{R_c^2+R^2}}\arctan\left(\frac{z/q}{\sqrt{R_c^2+R^2}}\right) \tag{4}$$

$$= \frac{V_{h,\infty}^2\sqrt{1-q^2}}{2\pi G\sqrt{R_c^2+R^2}\,\arccos q}\arctan\left(\frac{z/q}{\sqrt{R_c^2+R^2}}\right), \tag{5}$$

with $V_{h,\infty}$ the asymptotic rotation velocity of the round dark halo. Since $V_{h,\infty}$ is roughly proportional to the Galactic rotation speed, we find that the dark halo column density is proportional to Θ_0^2. At the Solar circle, and for $z = 1.1$ kpc, equation (5) can be approximated:

$$\frac{\Sigma_{h,1.1}(q)}{\Sigma_{h,1.1}(1)} \approx 1.1R_0 \;+ R_0\,(0.9 - R_0)\,q \qquad q \lesssim 0.15 \tag{6}$$

$$\approx \quad q^{-13/20} \qquad\qquad\qquad\qquad q \gtrsim 0.15 \tag{7}$$

where the core radius has been set to R_0. The total mass is found by adding the components: $\Sigma_{1.1}^{tot} = \Sigma_{h,1.1}(q) + \Sigma_{ISM} + \Sigma_*$. If we use the fiducial values, $\Sigma_{1.1}^{tot}$=71, Σ_{ISM} = 14.5, and Σ_*=35 $M_\odot\,\mathrm{pc}^{-2}$, we can determine $\Sigma_{h,1.1}(q)$. Thus, there is $\sim$21.5 $M_\odot\,\mathrm{pc}^{-2}$of dark matter within 1.1 kpc of the Milky Way's plane. But note that if the true mass of the stellar disk differs from the assumed value, the total amount of dark matter will be different so as to add up to the observed total of 71 $M_\odot\,\mathrm{pc}^{-2}$. In principle, the dark matter can be in a round or highly flattened distribution, but the required halo shape will depend on the actual mass of the stellar disk. A massive stellar disk requires less dark matter in a rounder halo, while a low mass disk requires a more flattened halo. With the aid of the equations above, we can formalize these considerations.

If we define $\Sigma_* = 35 + \delta\Sigma_*$, use the fiducial values for $\Sigma_{1.1}^{tot}$, $\Sigma_{h,1.1}(q)$, and Σ_{ISM}, and apply equations (6) and (7), we can relate the required halo flattening to $\delta\Sigma_*$:

$$q \;\approx\; \frac{21.5 - R_0\,\Sigma_{h,1.1}(1) - \delta\Sigma_*}{0.9{R_0}^2\Sigma_{h,1.1}(1)} \tag{8}$$

$$\approx \left(\frac{\Sigma_{h,1.1}(1)}{21.5}\right)^{20/13}\left[1 + \left(\frac{20/13}{21.5}\right)\delta\Sigma_*\right] \tag{9}$$

for the same q-ranges as in Eqns. (6) and (7). Since $\Sigma_{h,1.1}(q=1)$ depends on Θ_0 [eqn. (5)], the solutions of equations (8) and (9) depend on R_0, Θ_0, and $\delta\Sigma_*$. We use our mass models to determine $\Sigma_{h,1.1}(R_0, \Theta_0; q = 1)$ and rewrite equations (8) and (9) for a few interesting cases. For $\delta\Sigma_* = 0$ we find:

$$q \;\approx\; 0.07 \pm 0.05 \qquad (\Theta_0 = 165) \tag{10}$$

$$q \;\approx\; 0.4 - 0.1(R_0 \;- 7.1) \pm 0.1 \qquad (\Theta_0 = 175) \tag{11}$$

$$q \;\approx\; 0.8 - 0.2(R_0 \;- 7.1) \pm 0.2 \qquad (\Theta_0 = 185) \tag{12}$$

Thus, lower rotation speeds and larger R_0's require more highly flattened halos. Furthermore, for any fixed value of R_0, the *slope* of the $q - \delta\Sigma_*$ relation depends strongly upon the flattening itself. For example, with R_0=7.1 kpc we find:

$$q \;\approx\; 0.069 + 0.005\,\delta\Sigma_* \qquad (\Theta_0 = 165) \tag{13}$$

$$q \;\approx\; 0.400 + 0.030\,\delta\Sigma_* \qquad (\Theta_0 = 175) \tag{14}$$

$$q \;\approx\; 0.800 + 0.060\,\delta\Sigma_* \qquad (\Theta_0 = 185) \tag{15}$$

Equations (10) through (15) clearly show that small values of the Galactic rotation speed imply a highly flattened dark matter halo, whatever our distance to the Galactic centre, and whatever the mass of the stellar disk. We also see that the last three relations constrain Σ_* rather tightly: for models with $\Theta_0 \lesssim 185$ km s^{-1}, an increase in the stellar column density of $\sim$10 $M_\odot\,\mathrm{pc}^{-2}$ covers the whole allowed range for q.

So far we have been considering the dark halo column as a function of the Galactic constants, q, and Σ_* for the illustrative example of $R_c = R_0$. More generally, we can determine q as follows. For each Galactic model – with given values of R_0, Θ_0, $h_{\rm R}$, and stellar mass – we find that the *total mass* within 1.1 kpc of the plane is well described by a power law relation with index α:

$$\Sigma^{tot}_{1.1}(q) \approx \Sigma^{tot}_{1.1}(q=1) \times q^{-\alpha} . \quad (16)$$

where α lies in the range $\sim 0.05 - 0.45$. We then calculate $\Sigma^{tot}_{1.1}(q)$ for several values of the halo flattening, and fit for α. The so-determined α-value and the observed value of $\Sigma^{tot}_{1.1}(q)$ ($= 71 \pm 6\ M_\odot\,{\rm pc}^{-2}$, KG91) yields q and its error. We determine $\Sigma^{tot}_{1.1}(q)$ for $q < 1$, but adopt the same procedure too determine q for the mildly prolate cases we encounter.

4.2 Constraints from the thickness of the gas layer

In an idealized picture, the equilibrium thickness of the gas in the Milky Way depends only on the gas temperature and the form of the potential in which it has settled. Thus, the observed full width at half maximum (FWHM) of the gas layer can be used to constrain the potential of the Galaxy. In the accompanying paper we present evidence that the interstellar medium beyond the optical disk comprises only a single, iso-thermal component. We therefore adopt the same assumption in the analysis below. In section 5 we will include non-thermal pressure gradients in equation (17).

If the gas layer is in a steady state and we assume that only thermal and random motions of the gas contribute to the pressure in the ISM, the thickness of the gas layer follows from the equation of hydrostatic equilibrium:

$$\frac{d\ \sigma_g^2 \rho_g(z)}{dz} = \rho_{\rm g}(z)\ K_{\rm z}(z) , \quad (17)$$

where σ_g and $\rho_g(z)$ are the gaseous velocity dispersion and volume density.

If one neglects the self-gravity of the gas, one finds a simple relation between the thickness of the gas layer and the dark matter density. Unfortunately, the self-gravity of the gas contributes ~50% to the total vertical force, so that the relations between the gas layer width and the DM density are more complicated. To overcome this problem, we present and calibrate a simple approximation which we will use to relate the observed gas layer widths to the DM density. Since the Galactic constants and the gaseous velocity dispersion are somewhat uncertain, we also investigate how the relations depend on the adopted values for these quantities. Unlike the stellar kinematical method, the thickness of the gas layer is insensitive to Σ_* (Olling 1995).

In the local approximation we can estimate $K_{\rm z}$ from equation (3), and determine the gas layer width if the potential is dominated by one mass component:

$${\rm FWHM} \propto \frac{\sigma_g}{\sqrt{4\pi G \rho}} . \quad (18)$$

The proportionality constant depends on the vertical density distribution of the dominant mass component (Olling 1995). If the self-gravity of the gas dominates we can write:

$${\rm FWHM}_{self} \approx 0.159 \frac{\sigma_g^2}{\Sigma_g} , \quad (19)$$

where Σ_g is the gaseous surface density in $M_\odot\,{\rm pc}^{-2}$, and σ_g in km s^{-1}. In the case where the dark matter halo dominates the potential, we find:

$${\rm FWHM}_{halo} \approx \sqrt{\frac{13.5\ q}{1.4+q}} \frac{\sigma_g}{V_{\rm h,\infty}} \sqrt{R_{c,1}^2 + R^2} , \quad (20)$$

where $R_{c,1}$ is the core radius of the round halo, and with all distances are in kpc, and $V_{\rm h,\infty}$ in km s^{-1}. Taking $V_{h,\infty} \approx \Theta_0$ and and assuming that $R_c^2 << R^2$, we can solve equation (20) for q:

$$q \approx \frac{1.4(\alpha\Theta_0)^2}{13.5\sigma_g^2 - (\alpha\Theta_0)^2} , \quad (21)$$

with $\alpha = {\rm FWHM}/R$ (~ 0.07 for the Milky Way). As mentioned above, all mass components contribute to the potential so that the relation between the observed thickness, Θ_0, σ_g, and q are more complicated than in equation (21). Following Olling (1995) we approximate the true gas layer width as a superposition of the individual cases. As the relative density of the mass components depend on radius, their relative importance depends on radius as well:

$$\left(\frac{1}{{\rm FWHM}_{obs}(R)}\right)^2 \approx \sum_i \left(\frac{w_i(R)}{{\rm FWHM}_i(R)}\right)^2 , \quad (22)$$

where the weighting factors $w_i(R)$ are varied according to the contribution of component i to the total column density. In Table 1 we identified the mass models for which we calculate the model gas layer widths correctly. Using these models, we determine the values for $w_i(R)$ that best reproduce the exact gas layer thickness. The approximation of equation (22) matches the exact calculations to within 3% beyond the truncation of the stellar disk.

The analytic model presented above shows that inferred halo flattening depends on the amplitude of the Galactic rotation curve [eqn. (21)]. Furthermore, the observed H I widths scale with R_0 (Paper 1), so that flaring observations can be used to constrain both Galactic constants. In Paper I we showed that, for many combinations of parameters, a round halo is too dense to explain the observed flaring. Albeit not entirely correct, we will determine the halo's contribution to equation (22) from equation (20) in those cases. The halo's flattening is then determined from a fit to the extended FWHM-q sequence. In the next section we investigate how the halo's flattening and the stellar column density depend upon R_0, Θ_0, and σ_g employing the approximations presented above.

5 EFFECTS OF A LARGER GASEOUS VELOCITY DISPERSION

Above we argued that stellar kinematical data in combination with H I flaring measurements place limits on the Galactic constants, the mass of the stellar disk and the shape of the halo. In section 3 we discussed the strength of the constraint on our models due to the observed mass of the stellar disk. From our analytical approximation to the true gas layer width [eqn. (20)], we see that the model flaring of the gas layer also depends the velocity dispersion of the gas. If we are to use the observed flaring to constrain the mass models, we need to consider the impact of the uncertainty in σ_g.

The dark halo flattening inferred from the gas layer flaring ($q_{\rm H\ I}$) is approximately independent of Σ_*. Conversely, the halo's axial ratio inferred from the stellar kinematics ($q_{1.1}$) increases with increasing Σ_* [eqns. (13)-(15)]. For a given combination of Galactic constants, a Galactic mass model is self-consistent only if $q_{\rm H\ I}$ equals $q_{1.1}$. Thus, the combination of the flaring and stellar kinematical data result in a tight constraint on the local stellar column density. However, equations (20) and (21) shows that smaller gaseous velocity dispersions and larger values for Θ_0 require a rounder halo ($q_{\rm H\ I}$ larger). Thus, strong inter-relations exist between the Galactic constants, Σ_*, and the halo's flattening.

The above arguments imply that a change in the gaseous velocity dispersion will not affect the $q_{1.1}(\Sigma_*)$ relation, but will change $q_{\rm H\ I}$ so that the self-consistent mass model will have a different stellar disk mass and dark halo flattening. Thus, the analysis presented in Paper I could be compromised if the true gaseous velocity dispersion differs from the assumed value of 9.2 km s^{-1}. In the same paper we showed that a round halo is not of sufficiently low density to explain the flaring of the gas layer if we use the IAU recommended values for the Galactic constants ($R_0 = 8.5$ kpc, $\Theta_0 = 220$ km s^{-1}). Using the local approximation [eqn. (22)], we find that a round dark matter halo is consistent with the observed flaring and the IAU values if the gaseous velocity dispersion in the outer Galaxy is $\sim$17% larger. However, observations of external galaxies imply that the velocity dispersion declines slightly in the radial range over which the Milky Way's flaring has been measured, by a factor 1.12 $\pm$ 0.12 (van der Kruit & Shostak 1984; Dickey, Hanson & Helou 1990; Kamphuis 1993; Olling 1996b; Sicking 1997). An increase in gaseous velocity dispersion beyond the Solar circle is thus not a likely explanation for the discrepancy between model predictions and the observed flaring for the case of the IAU recommended Galactic constants. We come back to this issue in §5.2.

5.1 Non-thermal pressure terms

In Paper 1 and section 4.2 above we argued that the ISM beyond the optical disk comprises a single, iso-thermal component. We now investigate the possibility that non-thermal pressures have to be included in the hydrostatic balance.

It is estimated that in the Solar neighbourhood thermal motions, cosmic rays, and magnetic fields contribute about equally to the interstellar pressure (Spitzer 1978; Kulkarni & Heiles 1988). The equation of hydrostatic equilibrium can than be written as follows:

$$\frac{dP_G}{dz} + \frac{dP_B}{dz} + \frac{dP_C}{dz} = \rho_{\rm g}(z)\ K_{\rm z}(z) \quad (23)$$

$$(\sigma_g')^2 \frac{d\rho{\rm g}}{dz} = \rho_{\rm g}(z)\ K_{\rm z}(z) \quad (24)$$

with $P_G = \sigma_g^2 \rho_g(z)$ the thermal gas pressure, $P_B = B^2/8\pi$ is the magnetic field pressure, and $P_C = 1/3 U_C$ is the pressure due to cosmic rays with energy density U_C, and σ_g' the effective velocity dispersion. Following Spitzer we define $\alpha = P_B/P_G (\sim 0.25)$ and $\beta = P_C/P_G (\sim 0.4)$ and assume that they have the same vertical gradients. Comparing the results with equation (18), we find that the 'non-thermal gas layer widths' (FWHM$_{GBC}$) equals $\sqrt{1+\alpha+\beta} (\sim 1.28)$ times the 'thermal widths' (FWHM$_G$). In this case, the effective velocity dispersion equals $\sqrt{1+\alpha+\beta}$ times σ_g. However, the scale-heights of the B-field and the cosmic ray energy density may be as much as 2.5 kpc and 1 kpc, respectively (eg; Kulkarni & Heiles 1988; Rupen 1991). Since these scale-heights are, respectively, about 10 and 4 times lager than the scale-height of the H I, the non-thermal pressure *gradients* which occur in equation (23) are strongly reduced so that we arrive at: FWHM$_{GBC} \approx \sqrt{1+\alpha/10+\beta/4} \times$ FWHM$_G \sim 1.06 \times$ FWHM$_G$.

With respect to the pressure at the Solar circle, the gas pressure in the outer Galaxy is reduced by a factor of about 4, as a result of the decrease in column density (factor 2) and the increase in scale-height (factor 2). To make a conservative estimate as to the importance of the non-thermal terms at large distances, we assume that P_B and P_C and their vertical gradients have the same values as in the Solar neighbourhood. Thus, $P_{tot}(2R_0) = (0.25+\alpha+\beta) \times P_G(R_0)$. As a result of the increase in the scale-height of the thermal pressure and the assumed constancy of the scale-height of the non-thermal pressures, the relative importance of the former decreases, and we find:

$$\frac{\rm FWHM_{GBC}}{\rm FWHM_G} \approx \sqrt{1 + \frac{\alpha}{5*0.25} + \frac{\beta}{2*0.25}} \quad (25)$$

$$\approx \sqrt{1+0.2+0.8} \sim 1.4 \quad (26)$$

Based on the arguments above one might expect that non-thermal pressure gradients could dominate the hydrostatic balance in the outer parts of the Milky Way. Therefore, the non-thermal components of the pressure could significantly influence the interpretation of the H I gas layer widths.

However, the vertical balance is only affected if the magnetic field is horizontally stratified, a configuration that is unstable (Parker 1966), and which is thus not expected to exist on a global scale in the Milky Way. Similarly, the contribution from cosmic ray pressure is also likely to be localized because high cosmic ray fluxes are closely associated with the sites of star formation (Bicay & Helou 1990), which are rare beyond the optical disk.

Furthermore, there is evidence that non-thermal pressure support is small even when simplified calculations [cf.

eqn. (23)] indicate that they may dominate P_G. Observations of two external galaxies with very similar luminous mass distribution and rotation curve, NGC 891 & NGC 4565, indicate that non-thermal effects are negligible. Using a plane-parallel magnetic field configuration of which the strength is estimated from the radio continuum flux, Rupen (1991) estimates that the non-thermal pressure gradients equal 400% of the thermal pressure gradient in NGC 891, and 50% in NGC 4565. If non-thermal effects were important we would expect very different gas layer widths. In fact, these two galaxies have almost indistinguishable flaring gas layers (Rupen 1991), and we can conclude that thermal pressure gradients dominate (Olling 1996a).

To summarize, simplified theoretical considerations indicate that non-thermal pressure support could dominate the hydrostatic balance, while provisional observational data suggests the contrary. Below we seek to resolve this situation by lumping our ignorance of the actual value of the gaseous velocity dispersion and the non-thermal support into the effective velocity dispersion parameter σ_g' and use equation (24) to determine the model gas layer widths. Based on the arguments presented above, we expect σ_g' to lie between $\sim$0.85 and $\sqrt{2}$ times the default value of 9.2 km s^{-1}.

5.2 Constraints on the pressure term

We thus follow the procedure outlined in Paper I to see how our conclusions with regard to the interrelations between the Galactic constants, Σ_* and q are affected by the choice of σ_g'. In essence, we calculate the parameters of the self-consistent Galactic mass models for a range in effective velocity dispersions and many combinations of the Galactic constants. That is to say, we determine $\Sigma_*(R_0, \Theta_0, \sigma_g')$, and $q(R_0, \Theta_0, \sigma_g')$. The results, contoured in Fig. 3, indicate that the inferred halo flattening and stellar column density are very sensitive to the adopted value of σ_g'.

Let us first examine the cases with an effective dispersion larger than the default value of 9.2 km s^{-1} (upper panels). All else being equal, a larger gaseous velocity dispersion means that the model gas layer widths will be larger. To be consistent with the observed thickness, a larger K_z (more matter close to the plane) is required. Thus, for a given R_0 & Θ_0, a more highly flattened DM halo and hence a smaller $q_{\rm H\ I}$-value is found. A smaller $q_{\rm H\ I}$ also requires a smaller $q_{1.1}$, and hence a smaller Σ_* [cf. eqns. (13)-(15)]. Such lower values of q and Σ_* are seen in Fig. 3 for the $\sigma_g'/\sigma_g > 1$ cases (upper panels). From this figure we also see that the mass of the stellar disk constrains the value of σ_g'.
For example, if σ_g' were as large as 10.5 km s^{-1} (upper left panel), the KG89 value of Σ_*=35 $\pm$ 5 $M_\odot\,{\rm pc}^{-2}$ effectively rules out all Galactic constants considered, while for the GBF97 value of Σ_*=25.8 $\pm$ 3.8 $M_\odot\,{\rm pc}^{-2}$, or for our suggested column of 32 $\pm$ 11 $M_\odot\,{\rm pc}^{-2}$, essentially all values for R_0 are allowed, while this requires $\Theta_0 \lesssim 210$ km s^{-1}. Values for σ_g' that are as much as 30% larger than the default value (upper right panel of Fig. 3) are completely excluded because of the very small stellar disk masses required.

For lower velocity dispersions we expect the opposite trend. For given Galactic constants, larger q-values and stellar columns should be found. Above $\Theta_0\sim$175 km s^{-1}, this is indeed what is observed in Fig. 3 (lower left panel). For smaller values of Θ_0, the situation appears to be more chaotic, which is easily understood. On the one hand, a smaller velocity dispersion requires large $q_{\rm H\ I}$ values, but below $\Theta_0\sim$175 km s^{-1}, the rotation curve and the $\Sigma_{1.1}^{tot}$-constraint require small $q_{1.1}$-values [see §2, below equation (5)]. Furthermore, $q_{1.1}$ becomes almost independent of Σ_* in this regime. Thus, below $\Theta_0\sim$175 km s^{-1}, the "Gas Layer Flaring" and the "Stellar Kinematics" methods provide mutually exclusive constraints, so that no self-consistent models can be found. This inconsistency is reflected by the large negative values for Σ_* and q in the lower left panel of Fig. 3. In fact, an effective velocity dispersion $\lesssim 8$ km s^{-1} is essentially ruled out.

In order to take all constraints properly into account, we should be presenting a three dimensional plot with R_0, Θ_0 and σ_g' as the axes. Because this is a little tedious to present, we opt for another approach. In Paper I, we have considered three sets of Galactic constants, which are all consistent with the constraint set by the Oort constants: A-B= $\Theta_0/R_0 = 25.9$ km s^{-1} kpc^{-1}. This value is consistent with Kerr & Lynden-Bell's value of 26.4 ± 1.6 km s^{-1} kpc^{-1} (1986). We therefore determine the halo flattening and Σ_* along the line $\Theta_0 = 25.9 \times R_0$, for a series of gaseous velocity dispersions, and contour the results in Fig. 4. The fat horizontal bar in this figure represents our best estimate for R_0 as determined from the Oort functions (Olling & Merrifield 1997a,1998b). It is very satisfactory to see in Fig. 4 that the entirely independent analysis of the Oort functions yields values for Galactic constants that are fully consistent with the column density and velocity dispersion constraints derived above. With the value for R_0 as determined from the Oort functions, the gaseous velocity dispersion for the inner Galaxy [vertical bar, (Malhotra 1995)], and the requirement that the dark halo is oblate, we find that the Milky Way's dark halo has an axial-ratio larger than $\sim$0.35, and that $20 \lesssim \Sigma_* \lesssim 40\ M_\odot\,{\rm pc}^{-2}$.

The Kuijken & Gilmore (1989) estimate of the mass of the stellar disk in combination with the oblateness constraint (dark shaded region in Fig. 4) requires $R_0 \lesssim 7.8$ kpc, $8 \lesssim \sigma_g' \lesssim 10$ km s^{-1}, and probably an almost round halo. If the mass of the stellar disk is as low as proposed by Gould, Bahcall & Flynn (1997; the lightly shaded region in Fig. 4), values of R_0 up to 8.4 kpc are allowed. If no constraint on the halo shape is imposed, our suggested value for Σ_*= 32 $\pm$ 11 $M_\odot\,{\rm pc}^{-2}$ implies a firm upper limit to the halo flattening of $q \lesssim 1.6$. Significantly flattened dark halos ($q \lesssim 0.4$) are only allowed if $R_0 \lesssim 7.1$ kpc. With the same column density constraint, and if $R_0 \geq 7.1$ kpc, the gaseous velocity dispersion in the outer Galaxy and R_0 are tightly correlated: $\sigma_g' = [9.2 + 0.7 \times (R_0 - 7.1)] \pm 0.6$ km s^{-1}. Highly flattened dark matter halos and a significant non-thermal pressure support for the H I layer are consistent with the data only if $R_0 \lesssim 6.8$ kpc.

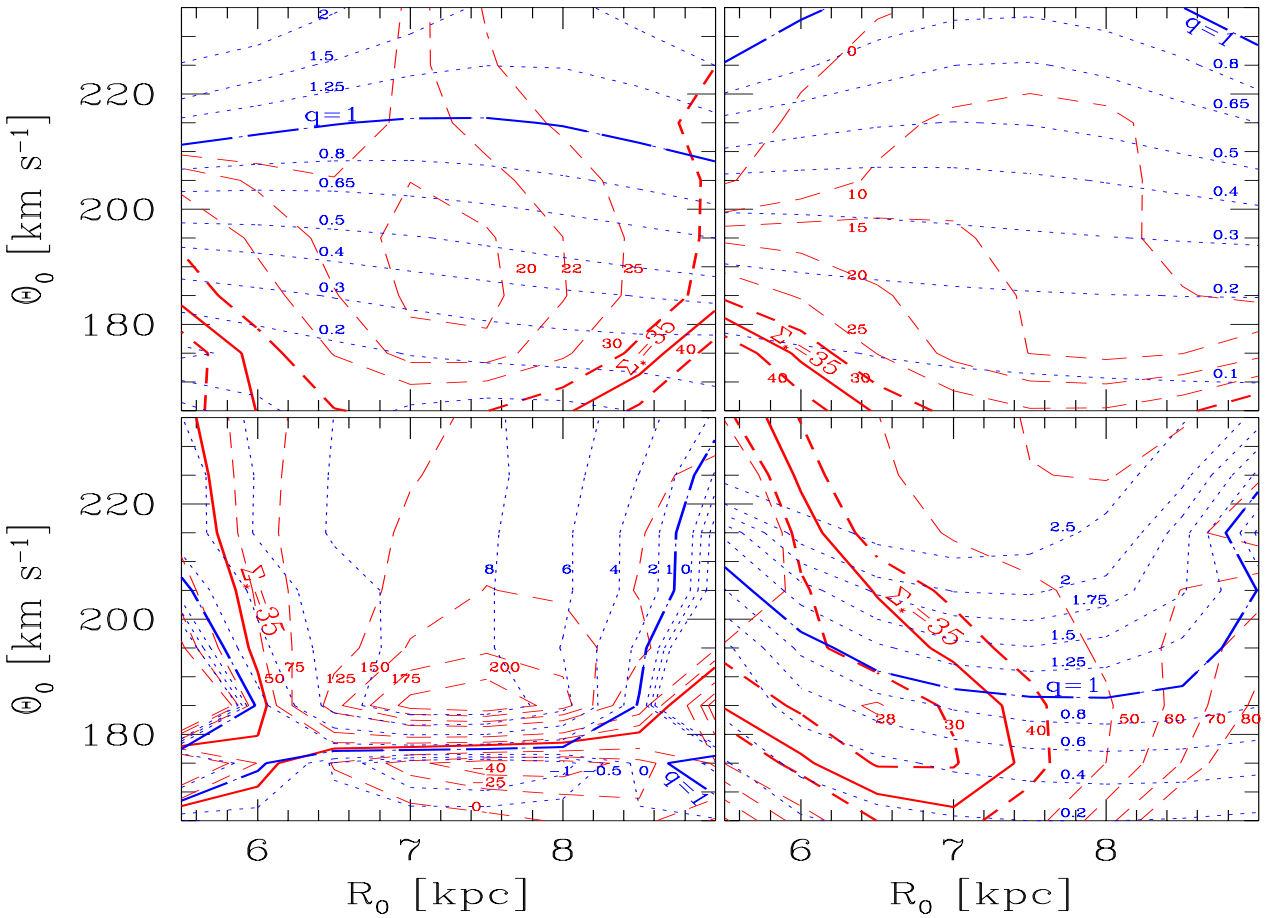

Figure 3. Here we present the *mutually consistent* set of Galactic constants, stellar column density in the Solar neighborhood (Σ_*; long dashed lines) and halo flattening (q; dotted lines). The individual panels show the results of the calculation for several values of σ'_g/σ_g: 0.85 (σ'_g=8 km s^{-1}, lower left), 1.0 (σ'_g=9.2 km s^{-1}, lower right), 1.15 (σ'_g=10.5 km s^{-1}, upper left), and 1.30 (σ'_g=12 km s^{-1}, upper right). The oblate-prolate boundary is indicated by the heavy dash-dotted line. The heavy full line and the heavy dashed line corresponds to KG89's determination of Σ_*, and the $\pm1-\sigma$ values. The upper limit of GBF97's determination of the stellar column density corresponds to the $\Sigma_*\sim$ 30 $M_\odot$ pc^{-2} contour. Both the halo flattening and stellar column are determined to $\sim$ 6% accuracy. Because the Galactic constants, Σ_*, and q are mutually consistent one cannot arbitrarily choose the four parameters. Fixing one of the four parameters severely restricts the other three. Any two parameters follow immediately from any choice of the other two.

6 SUMMARY AND CONCLUSIONS

In Paper I we showed that the constraints on the dark matter density in the Solar neighbourhood and the outer Galaxy place tight limits on the choice of the Galactic constants (R_0 & Θ_0), the mass of the stellar disk (Σ_*), and the dark halo's flattening (q). In this paper we present the analytical tools that allow for an efficient search through parameter space. Employing these tools, we extend the analysis by investigating the effects of the unknown gaseous velocity dispersion on the gas layer flaring constraint and the effects on the inferred values for R_0, Θ_0, Σ_*, and q. The strongest constraints available are the observed Θ_0/R_0 ratio, the mass of the stellar disk and the fact that the dark halo is almost certainly oblate. Taken together, these constraints rule out any substantial contributions to the support of the H I layer beyond the optical disk by cosmic ray pressure and magnetic fields (Fig. 4). We find that the Milky Way's dark matter halo is close to spherical for all but the smallest values of R_0. Using Kuijken & Gilmore's determination of the mass of the stellar disk, we find upper limits to the Galactic constants: $R_0 \lesssim 7.8$ kpc, and $\Theta_0 \lesssim 202$ km s^{-1}. A significantly flattened dark matter halo is only possible if our distance to the Galactic centre is smaller than $\sim$ 6.8 kpc.

The strong correlations between the mass models' parameters limit our ability to freely choose those parameters. For example, it is only possible to construct a self-consistent oblate model of the Galaxy based on the IAU-recommended values for the Galactic constants ($R_0 = 8.5$ kpc, $\Theta_0 = 220$ km s^{-1}) if the local stellar column density is less than about 22 $M_\odot$ pc^{-2}, and $\sigma'_g \gtrsim 10.8$ km s^{-1}.

The existence of the "vertical disk-halo conspiracy", de-

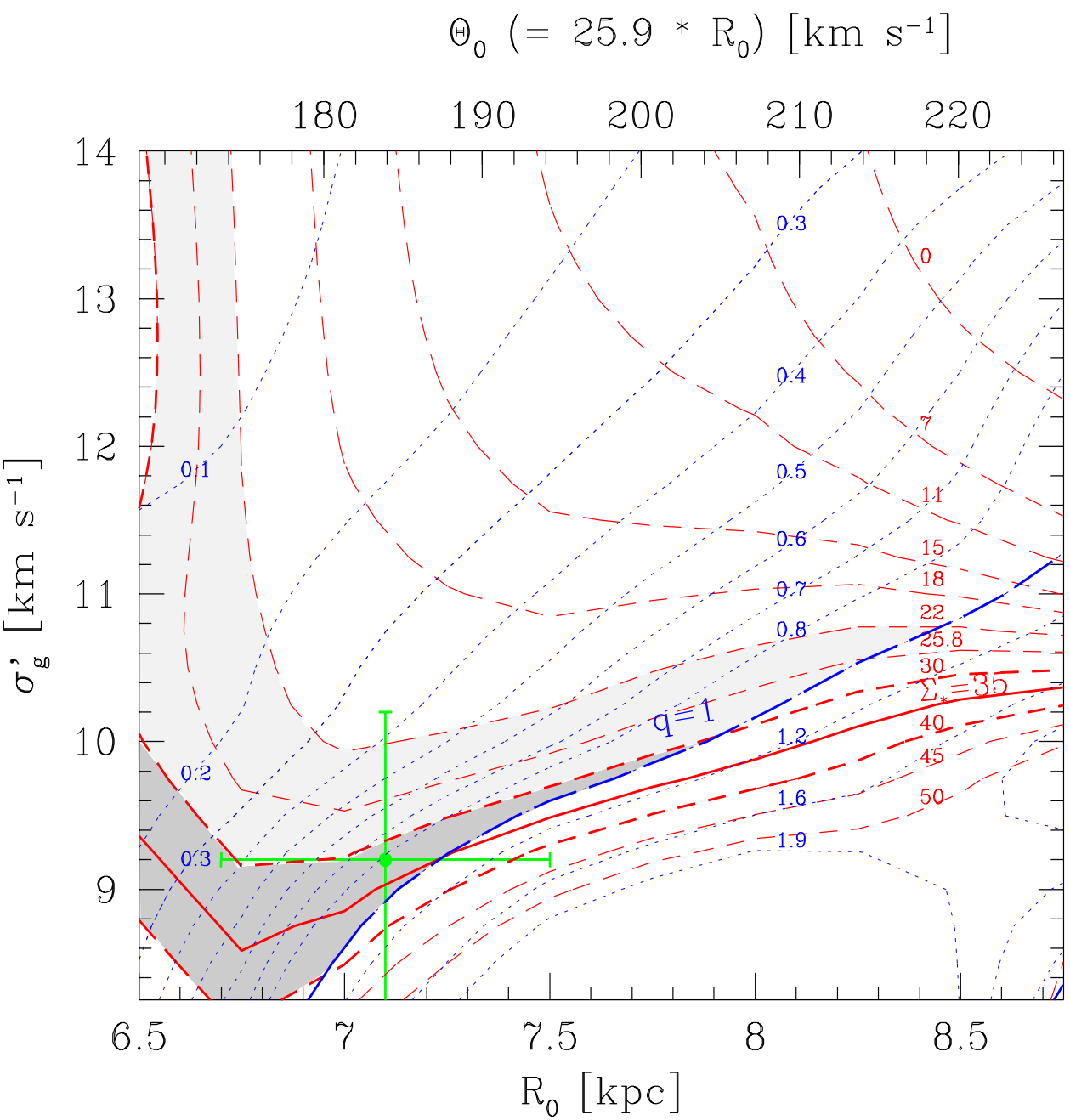

Figure 4. In this figure we present the interrelations between the adopted value of the gaseous velocity dispersion (σ'_g) and the Galactic constants. The line coding is the same as in Figs. 3. This figure was generated by extracting the halo flattening and Σ_* values along the line $\Theta_0 = 25.9 \times R_0$, for several values of the effective gaseous velocity dispersion. The fat cross represents our best estimate for the Galactic constants [$R_0 = 7.1 \pm 0.4$ kpc, $\Theta_0 = 188 \pm 8$ km s^{-1}, (Olling & Merrifield 1997a,1998b)], and the gaseous velocity dispersion [$\sigma_g = 9.2 \pm 1$ km s^{-1}, (Malhotra 1995)]. Large effective velocity dispersions require flattened halos. Round, and even prolate, halos are found for small σ'_g values. In the shaded region of parameter space, the dark halo is oblate, and the mass of the stellar disk is as measured by KG89 (dark shading) and GBF97 (light shading). Choosing the IAU R_0 & Θ_0 values results in strong correlations between the remaining three parameters of the mass model, we find: $q_{\rm IAU} \sim 0.62 - 0.31(\sigma'_g - 11.9) + 0.11(\sigma'_g - 11.9)^2$ and $\Sigma_{*,\rm IAU} \sim 16 - 17(\sigma'_g - 11.1) + 4.8(\sigma'_g - 11.1)^2$.

scribed in section 3, means that stellar kinematical data above $\sim$1 kpc are required in order to distinguish between the different possible vertical density profiles. Kuijken & Gilmore's (1991) determination of the column density of matter within 1.1 kpc of the plane ($71 \pm 6\ M_\odot\,\mathrm{pc}^{-2}$) is robust and valid over a wide range of Galactic constants. For the contribution to this total mass from the stellar disk, we suggest an observational consensus average of $32 \pm 11\ M_\odot\,\mathrm{pc}^{-2}$. But note that constraints on the halo shape or allowed ranges in σ_g' can limit Σ_* even further.

If $R_0 \gtrsim 7$ kpc, then the dark halo of the Milky Way is fairly close to spherical, and so we can already make some statements about the nature of the dark matter. In particular, the possibility that the dark matter is made up of decaying massive neutrinos (Sciama 1990) is ruled out. In that model, the dark matter is made up of a disk of massive neutrinos, whose decay is responsible for ionizing the interstellar gas. To maximize the ionization, the putative disk of massive neutrinos must be highly flattened [$q \sim 0.2$, (Sciama 1990)], which is not consistent with the constraints set above. Similarly, the possibility that the dark matter is made up of a flattened disk of cold molecular hydrogen (Pfenniger, Combes & Martinet 1994), for which $q \lesssim 0.2$, is ruled out. Since all other baryonic dark matter candidates have already been observationally excluded (Hegyi & Olive 1986), we must conclude that the dark matter halo of the Milky Way is most likely made up of something altogether more exotic (MACHOs, WIMPS, axions, neutralinos ...). Even in the Solar neighborhood, there are non-negligible quantities of this material: our proposed dark halo models imply that it amounts to some 0.25 GeV/c^2 per cubic centimetre or 0.0066 $M_\odot\,\mathrm{pc}^{-3}$. The direct detection of this material remains a challenge for experimental physicists.

ACKNOWLEDGEMENTS

We thank Andy Newsam, Irini Sakelliou, Konrad Kuijken, Marc Kamionkowski, Jacqueline van Gorkom, and the referee for useful discussions.

REFERENCES

Bahcall J.N., 1984a, ApJ, 276, 156
Bahcall J.N., 1984b, ApJ, 276, 169
Becquaert J.F., Combes F., Viallefond F. 1997, A&A, 325, 41
Begeman K., 1989, A&A, 223, 47
Begeman K., 1987, Ph. D. Thesis, University of Groningen
Bergstrom L., Ullio P., Buckley J.H., 1997, astro-ph/9712318
Bicay M.D. & Helou G., 1990, ApJ, 362, 59
Bienaymé O., Robin A.C. & Crézé M., 1987, A&A, 180, 94
Bottema R., 1993, A&A, 275, 16
Bronfman L., Cohen R.S., Alvarez H., May J. & Thaddeus P., 1988, ApJ, 324, 248
Burton W.B., 1988, in Verschuur G.L., Kellermann K.I., eds, Galactic and Extragalactic Radio Astronomy, p. 295
Bosma A., 1981, AJ, 86, 1825
Broeils A., 1992, Ph. D. Thesis, University of Groningen
Casertano S., van Gorkom J.H., 1991, AJ, 101, 1231
Crézé M., Chereul E., Bienaymé O., Pichon C., 1998, A&A, 329, 920
Crézé M., Robin A.C. & Bienaymé O., 1989, A&A, 211, 1
Dehnen W., Binney J., 1998, MNRAS, 294, 429
Dickey J.M., Hanson M.M. & Helou G., 1990, ApJ, 352, 522
de Jong R.S., 1996, A&A, 313, 45
Gould A., Bahcall J.N., Flynn C. 1997, ApJ, (GBF97)
Kamphuis J., 1993, Ph.D. Thesis, University of Groningen
Kulkarni S.R., & Heiles C., 1988, in Verschuur G.L., Kellermann K.I., eds, Galactic and Extragalactic Radio Astronomy, p. 95
Flynn C., Fuchs B., 1994, MNRAS, 270, 471
Freudenreich, H.T., 1998, ApJ, 492, 495
Freudenreich, H.T., 1996, ApJ, 468, 663
Gates E.I., Gyuk G., Turner M.S., 1995, PhRvL, 74, 3724
Hegyi D. & Olive K.A., 1986, ApJ, 303, 56
Kent S.M., 1992, ApJ, 387, 181
Kent S.M., 1987, AJ, 93, 816
Kent S.M., Dame T.M. & Fazio G., 1991, ApJ, 378, 131
Kuijken K. & Gilmore G., 1991, ApJ, 367, L9 (KG91)
Kuijken K. & Gilmore G., 1989b, MNRAS, 239, 605 (KG89)
Kuijken K. & Gilmore G., 1989a, MNRAS, 239, 571
Lake G., Feinswog L., 1989, AJ, 98, 166
Malhotra S., 1995, ApJ, 448, 138
McGaugh S.S., de Blok W.J.G., 1998, ApJ, accepted for publication, astro-ph/9801123
Navarro J., Frenk C.S., White S.D.M., 1996, ApJ, 462, 563
Olive K.A., Steigman G., 1995, ApJS, 97, 490
Olling R.P., Merrifield M.R., 1998a, submitted to MNRAS (Paper I)
Olling R.P., Merrifield M.R., 1998b, accepted for publication in MNRAS (astro-ph/9802034)
Olling R.P., Merrifield M.R., 1997a, in the proceedings of the Santa Cruz' "Galactic Halos" workshop, astro-ph/9711157
Olling R.P., Merrifield M.R., 1997b, in the proceedings of the Santa Cruz' "Galactic Halos" workshop, astro-ph/9710224
Olling R.P., 1997c, in Klapdor-Kleingrothaus H.V., Ramachers Y., eds, "Aspects of Dark Matter in Astro- and Particle Physics", p. 44, World Scientific, *astro-ph/9612018*
Olling R.P., 1996a, AJ, 112, 481-490
Olling R.P., 1996b, AJ, 112, 457-480
Olling R.P., 1995, AJ, 110, 591
Parker E.N., 1966, ApJ, 145, 811
Persic M., Salucci P., Stel F., 1996, MNRAS, 281, 27
Pfenniger D., Combes F., & Martinet L., 1994, A&A, 285, 79
Robin A.C., Crézé M. & Mohan V., 1992, ApJ, 400, L25
Rubin V.C., Ford W.K., Thonnard N., 1980, ApJ, 238, 471
Rupen M.P., 1991, Ph. D. Thesis, Princeton University
Sackett P.D., 1997, ApJ, 483, 103
Sackett P.D., Sparke L.S., 1990, ApJ, 361, 408
Sancisi R., Allen R.J., 1979, A&A, 74, 73
Sciama D., 1990, MNRAS, 244, 1
Sicking F., 1997, Ph.D. Thesis, University of Groningen
Spitzer L., 1978, Physical Processes in the Interstellar Medium, John Wiley & sons (New York)
Albada T.S. van & Sancisi R., 1986, Phil. Trans. R. Soc. Lond. A., 320, 447
van Albada T.S., Bahcall J.N., Begeman K., Sancisi R., 1985, ApJ, 295, 305
van der Kruit P.C., 1988, A&A, 192, 117
van der Kruit P.C., 1981, A&A, 99, 298
Shostak S., van der Kruit P.C., 1984, A&A, 132, 20